scientific reports

Check for updates

OPEN

An in vivo rat model for comparing selective blockade between sensory and motor nerve conduction

Yi Teng[1,3], Xian Zou[1,2,3], Jin Liu[1,2], Xiangyu Hu[1,2], Cheng Zhou[2] & Mengchan Ou[1]✉

Sensory-selective nerve blockade is highly useful for pain management in clinical practice, but developing such blockers remains challenging. A major handicap is the lack of objective in vivo animal models to evaluate motor and sensory nerve conduction simultaneously. Due to anatomical structures, motor evoked potentials (MEPs) and/or somatosensory evoked potentials (SSEPs) may be used to assess nerve conduction. MEPs were elicited by stimulating motor cortex and recorded from contralateral hind limb. SSEPs were generated by stimulating sciatic nerve and recorded from contralateral sensory cortex. Amplitude/latency changes were recorded under various physiological conditions (e.g., anesthesia, durations, temperatures, and oxygen) and drug interventions for validation. Compared to sevoflurane, propofol minimally inhibited MEPs at sedative doses and was therefore used during recordings. Both hypothermia (34–36 °C) and hyperthermia (38–40 °C) significantly suppressed MEP and SSEP amplitudes ($P < 0.0001$). Reduced oxygen saturation (SaO_2) decreased MEP amplitudes ($P < 0.0001$), and the amplitudes were strongly correlated with SaO_2 ($R^2 = 0.8284$). For selective blockade validation, lidocaine suppressed both MEP and SSEP amplitudes below 20% of baseline ($P < 0.0001$), confirming non-selectivity. In contrast, QX-314/capsaicin selectively suppressed SSEPs ($P < 0.0001$), while MEPs remained stable. This model is stable for evaluating selective nerve blockade in vivo for at least 60 min under controlled physiological conditions.

Keywords Selective nerve blockade, Evoked potentials, Sensory-motor separation, Local anesthetics, In vivo animal model

Local anesthetics are widely used in clinical settings, are regionally injected, and have few systemic side effects[1]. However, currently used local anesthetics have no selectivity between sensory and motor nerve blockade (e.g., lidocaine and bupivacaine), which limits their application in postoperative pain management. The ideal postoperative analgesic is a sensory-selective nerve blocker that blocks pain transmission while maximizing the retention of motor function to facilitate early mobilization[2]. A previous study showed that excessive motor blockade not only prolongs postoperative recovery time but also increases the risk of motor-related complications, such as deep vein thrombosis and lung infections[3]. Therefore, the development of novel local anesthetics that exhibit effective analgesia while preserving motor function is urgently needed for clinical anesthesia[4].

Currently, studies of local anesthetics primarily rely on neurobehavioral examinations. These studies mainly include assessing animal responses to thermal pain[5] and mechanical pain[6] to reflect the sensory nerve blockade effect, while methodologies such as Bioseb grip strength testing[7] and the extensor postural thrust test[8] are used to evaluate motor blockade. However, these behavioral methods are subjective and do not allow direct, precise, and quantitative analysis of nerve functions. The absence of an objective and reproducible in vivo model to simultaneously assess sensory and motor nerve conduction has limited the development of sensory-selective local analgesics. Thus, a standardized in vivo animal model is needed to evaluate sensory-motor selective blockade.

In clinical practice, motor-evoked potentials (MEPs) and somatosensory-evoked potentials (SSEPs) are widely used in neurosurgery, providing objective, quantitative, and real-time tools to evaluate neural conduction[9,10].

[1]Department of Anesthesiology, West China Hospital of Sichuan University, Chengdu, China. [2]Research Center of Anesthesiology, West China Hospital, Sichuan University, Chengdu, China. [3]Yi Teng and Xian Zou contributed equally to this work. ✉email: mengchanou@wchscu.edu.cn

This type of neurophysiological monitoring enables precise recording of neural pathway integrity, facilitating early detection of neuronal impairment during surgical procedures in the operating room. MEPs are used to assess descending motor pathways by stimulating the motor cortex and recording responses at peripheral muscles. In contrast, SSEPs are used to evaluate ascending sensory pathways by stimulating peripheral nerves and recording signals at the somatosensory cortex[11–13]. Given their distinct anatomical pathways, MEPs primarily reflect the conduction of descending motor fibers from the cortex to muscles, while SSEPs capture afferent sensory transmission from the periphery to the cortex. Theoretically, simultaneous MEP and SSEP recordings may enable functional dissection of motor and sensory pathways in vivo. Establishing an animal model integrating both MEPs and SSEPs thus may provide a reliable way to quantify sensory-motor selective nerve blockade in vivo.

In the present study, we developed an in vivo rat model that allows simultaneous and objective evaluation of sensory-motor blockade based on MEP and SSEP recordings. Specifically, the model was established by implanting stimulation and/or recording electrodes in the motor and sensory cortex, respectively. The influences of key physiological and pharmacological factors, including anesthesia, temperature, oxygenation, and recording duration, were evaluated. For model validation, we further tested the effects of lidocaine (a non-selective nerve blocker) and/or QX-314 combined with capsaicin (a sensory-selective combination). Overall, this model provides a robust experimental protocol for screening sensory-motor selective blockade.

Results

Sevoflurane suppresses MEP amplitude in a concentration-dependent manner

Screw electrodes were employed in the rat skull to elicit MEPs by applying electrical pulses to the motor cortex and recording from the contralateral tibialis anterior muscle (Fig. 1a). Similarly, SSEPs were induced by stimulating the sciatic nerve and recording from the contralateral sensory cortex (Fig. 1b). As the concentration of sevoflurane increased, the amplitude of MEPs gradually decreased. Representative MEP waveforms visually illustrate this concentration-dependent suppression (Fig. 1c). This decline became significant starting at about 0.60% ($P<0.001$ vs. baseline by two-way ANOVA, Fig. 1e). In contrast, the corresponding SSEP waveforms showed only subtle changes across the tested concentrations (Fig. 1d), with quantitative analysis confirming only a mild reduction at higher concentrations (Fig. 1f). The 50% and 95% inhibitory concentration (IC_{50} and IC_{95}, respectively) for MEP suppression were 0.52% and 0.96%, both markedly lower than the minimum alveolar concentration (MAC) of sevoflurane for inducing the loss of righting reflex[14] (~ 1.60%, Fig. 1g), indicating that motor pathways are more sensitive to sevoflurane than to general anesthetic depth.

Propofol attenuates MEP amplitude at doses higher than its sedative dose

Similarly, propofol reduced MEP amplitude in a dose-dependent manner (Fig. 2a), with a significant effect starting at 70 mg/kg/h ($P<0.01$ vs. baseline by two-way ANOVA, Fig. 2c). The calculated IC_{50} and IC_{95} for MEPs were 73.5 and 116.0 mg/kg/h, respectively, which were approximately two to three times higher than the median effective dose (ED_{50}) values that induced the loss of righting reflex[15] (~ 40 mg/kg/h, Fig. 2e). In contrast, SSEP amplitudes showed only a mild reduction across the same dose range (Fig. 2b,d). Given its relatively mild suppression of MEPs and minimal impact on SSEPs, propofol was selected as the preferred anesthetic agent for subsequent experiments. It was given by intravenous injection (10 mg/kg) and then maintained by continuous infusion (10–40 mg/kg/h) based on anesthetic depth.

MEPs and SSEPs are stable for at least 60 min under controlled body temperature

To evaluate the temporal stability of our models, we recorded MEP and SSEP signals at baseline, 30 min, and 60 min under stable anesthetic conditions while maintaining normothermia (36–38 °C) and continuous oxygen supplementation. Representative waveforms showed consistent appearances across these three time points for both MEPs (Fig. 3a) and SSEPs (Fig. 3c). Quantitative analysis further confirmed that, compared with the baseline, neither the amplitude nor latency of MEPs (Fig. 3b) or SSEPs (Fig. 3d) exhibited significant changes at 30 and 60 min ($P>0.05$), indicating reliable and stable electrophysiological recording throughout the 60-min period.

The impact of body temperature (hypothermia: 34–36 °C; normothermia: 36–38 °C; hyperthermia: 38–40 °C) on both MEP and SSEP recordings was then assessed. Representative waveforms showed notable changes in response to temperature alterations for MEPs (Fig. 3e) and SSEPs (Fig. 3h). Quantitative analyses revealed that both hypothermia and hyperthermia significantly reduced the amplitude of MEPs and SSEPs compared with those under normothermia ($P<0.0001$ by one-way ANOVA; Fig. 3f,i). Furthermore, non-linear regression analysis revealed a strong and significant relationship between body temperature and the amplitudes of both MEPs ($R^2 = 0.8385$, $P<0.0001$; Fig. 3g) and SSEPs ($R^2 = 0.7352$, $P<0.0001$; Fig. 3j). Additionally, hypothermia caused a slight but significant prolongation of MEP and SSEP latencies compared with those under normothermia ($P<0.05$ by one-way ANOVA; Fig. 3f,i), whereas hyperthermia did not significantly affect the latency ($P>0.05$ by one-way ANOVA; Fig. 3f,i). Collectively, these results suggest that both hypothermia and hyperthermia impair MEP and SSEP signals. Maintaining normothermic conditions (36–38 °C) is therefore essential for stable and accurate electrophysiological recordings.

MEP amplitude strongly correlates with blood oxygen saturation (SaO_2), whereas SSEP are minimally affected

To assess the impact of oxygen supply, we compared MEPs and SSEPs between animals receiving continuous oxygen (100% O_2) and room air (21% O_2). The MEP amplitude was significantly reduced in the air group compared with that in the oxygen group ($P<0.0001$ by unpaired t-test; Fig. 4a), with a strong positive correlation between SaO_2 and MEP amplitude (Spearman $r=0.8233$, $P<0.0001$ by simple linear correlation; Fig. 4b),

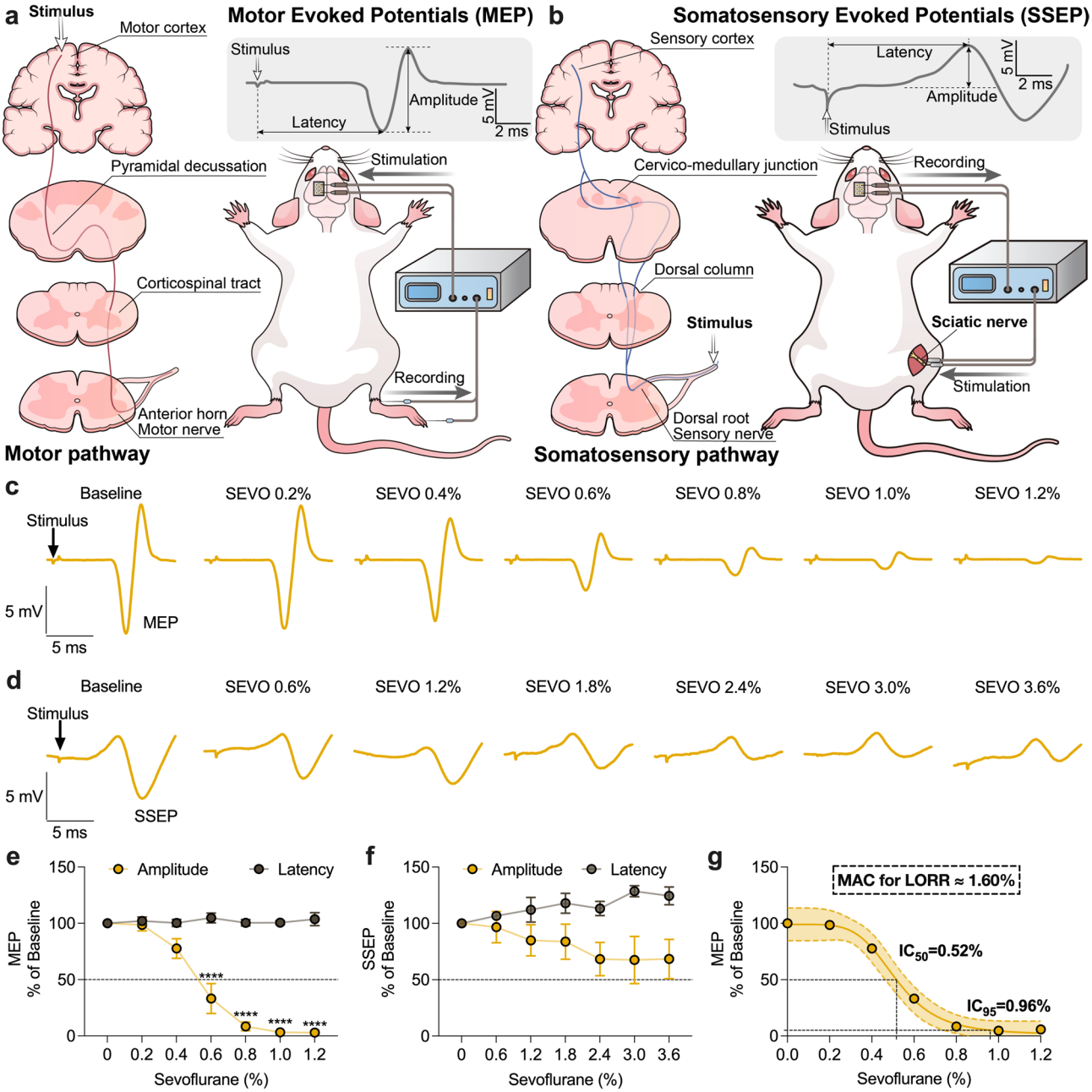

Fig. 1. Effects of different concentrations of sevoflurane on MEP and SSEP in rats. (**a,b**) Schematic diagrams illustrating the setup for MEP (**a**) and SSEP (**b**) recordings in rats. (**c,d**) Representative MEP and SSEP waveforms at baseline and after increasing concentrations of sevoflurane. (**e**) MEP amplitude significantly decreased in a dose-dependent manner starting at 0.6% sevoflurane, while latency remained unchanged ($n = 6$). (**f**) SSEP amplitude also decreased with increasing sevoflurane concentration, though less pronounced than MEP; latency gradually increased at higher doses ($n = 6$). (**g**) Dose-response curve of sevoflurane on MEP amplitude, showing $IC_{50} = 0.52\%$ and $IC_{95} = 0.96\%$, both below the MAC for LORR ≈ 1.8%. (**g**) Representative MEP waveforms under different doses of propofol. Data are shown as mean ± SD. Statistical analysis: two-way ANOVA (**e**,**f**) and nonlinear regression (**g**); statistical significance: $^{**}P < 0.01$, $^{****}P < 0.0001$ vs. baseline. IC_{50}, 50% inhibitory concentration; IC_{95}, 95% inhibitory concentration; MAC, Minimum alveolar concentration; LORR, loss of righting reflex; ED_{50}, median effective dose.

which was further confirmed by a robust linear regression association ($R^2 = 0.8284$, $P < 0.0001$ by simple linear regression; Fig. 4c). However, MEP latency remained unchanged ($P > 0.05$ by unpaired t-test; Fig. 4d), showing no significant correlation with SaO_2 (Pearson $r = 0.1458$, $P = 0.4966$ by simple linear correlation; Fig. 4e) and a weak regression association ($R^2 = 0.02126$, $P = 0.4966$ by simple linear regression; Fig. 4f). In contrast, for SSEPs, neither amplitude nor latency showed significant differences between the oxygen group and the air group ($P > 0.05$ by unpaired t-test; Fig. 4g,j), with no significant correlation or regression fit between SaO_2 and SSEPs

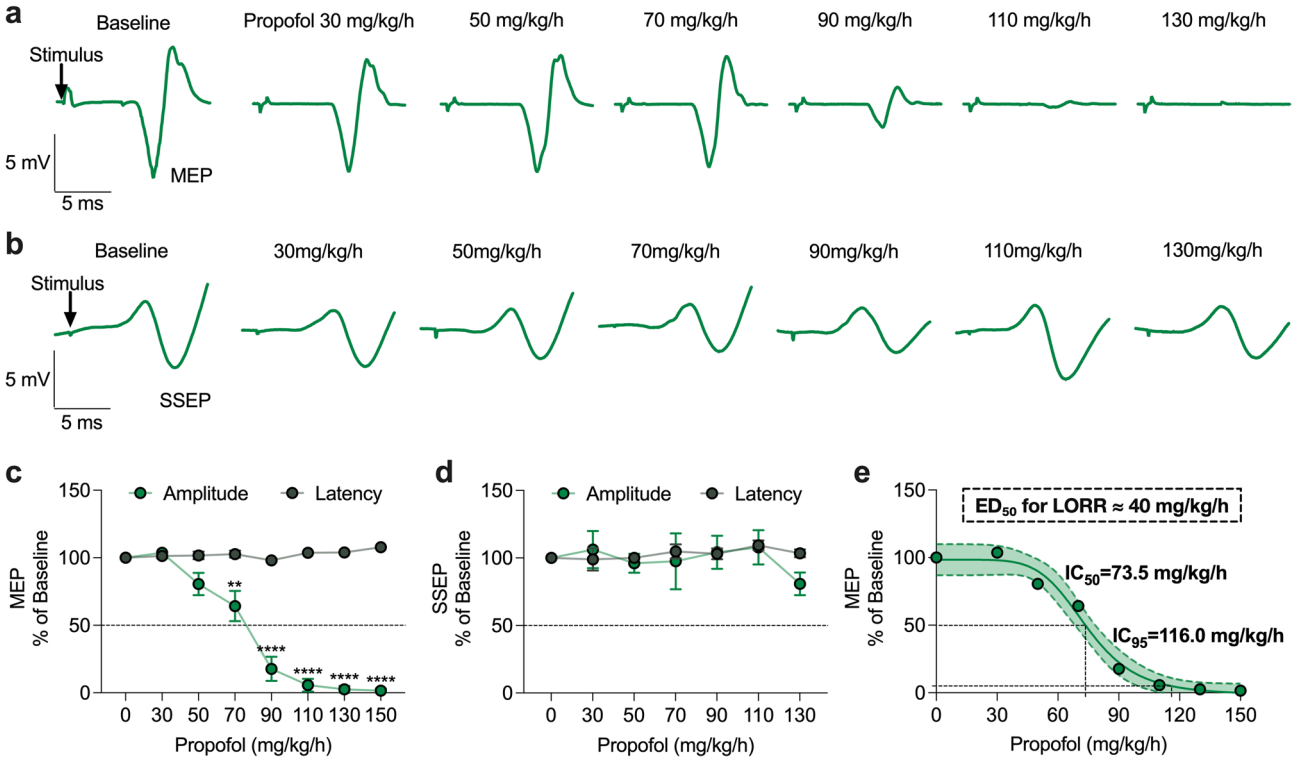

Fig. 2. Effects of different concentrations of propofol on MEP and SSEP in rats. (**a,b**) Representative MEP and SSEP waveforms at baseline and under different infusion doses of propofol. (**c**) Quantitative analysis of MEPs shows that amplitude was significantly reduced starting from 70 mg/kg/h, with no significant changes in latency ($n = 6$). (**d**) Quantitative analysis of SSEPs shows that both amplitude and latency remained stable under all tested propofol doses ($n = 6$). (**e**) Dose-response curve showing MEP inhibition by propofol, with $IC_{50} = 73.5$ mg/kg/h and $IC_{95} = 116.0$ mg/kg/h, both above the ED_{50} for LORR (≈ 40 mg/kg/h). Data are shown as mean ± SD. Statistical analysis: two-way ANOVA (**c**,**d**) and nonlinear regression (**e**); $^{**}P < 0.01$, $^{****}P < 0.0001$ vs. baseline. LORR, loss of righting reflex; ED_{50}, median effective dose.

(Fig. 4h,i,k,l). These findings suggest that oxygen supply plays a crucial role in maintaining MEP amplitude, while its effect on SSEP amplitude is weaker. Latency measurements for both MEPs and SSEPs appear to be less affected by oxygen availability.

Lidocaine non-selectively reduces both MEP and SSEP amplitudes

To investigate the effects of lidocaine on motor and sensory pathways in this model, we evaluated changes in MEPs and SSEPs following saline, 1% lidocaine, and 2% lidocaine injections. For MEPs, the amplitude was markedly suppressed after 1% and 2% lidocaine administration compared with that in the saline control ($P < 0.0001$ by one-way ANOVA; Fig. 5c,d), with unchanged latency ($P > 0.05$ by one-way ANOVA; Fig. 5c,d). For SSEPs, similarly, the amplitude exhibited a significant decline following lidocaine administration ($P < 0.0001$ by one-way ANOVA; Fig. 5e,f). Additionally, the SSEP latency was prolonged in both the 1% and 2% groups, with a greater increase at the 2% concentration (Fig. 5e,f). A comparison of MEP and SSEP amplitude trends highlighted a parallel reduction in response to lidocaine, whereas the SSEP latency showed a mild increase at higher concentrations (Fig. 5g,h). These findings validated that lidocaine non-selectively blocks both motor and sensory pathways. The greater effect on SSEP latency suggests that sensory conduction is more susceptible than motor transmission to lidocaine-induced delay.

To assess the reversibility and safety of lidocaine-induced blockade, we monitored evoked potentials at 5-minute intervals following 2% lidocaine administration until both MEP and SSEP amplitudes returned to baseline. Both signals began to recover within 20–30 min and were fully restored by 50 min (Fig. 5i). Furthermore, hematoxylin-eosin (HE) staining of dorsal root ganglia (DRG) and sciatic nerves harvested after lidocaine injection showed no detectable pathological alterations compared with saline controls, including absence of edema, inflammatory infiltration, axonal swelling, or myelin disruption (Supplementary Fig. S1a–d). These findings demonstrate that high-dose 2% lidocaine does not cause structural nerve damage and allows complete functional recovery of evoked potentials in this model.

QX314/capsaicin selectively decreases SSEP amplitudes but minimally suppresses MEPs over time

To assess the sensory-motor separation effect of QX-314 combined with capsaicin in vivo, we compared the changes in MEPs and SSEPs following perineural administration of saline, 10 mM QX-314/0.05% capsaicin,

and 20 mM QX-314/0.05% capsaicin. Because the onset time of QX-314 is slower than that of lidocaine, we measured signals at multiple time points (5, 10, 15, and 30 min) after administration.

We found both MEP amplitude and latency remained stable across all time points in all three groups, with no obvious changes compared with baseline, indicating that motor conduction was preserved (Fig. 6a–c, left). A quantitative comparison of the 30-minute time points further confirmed that the MEP amplitude and latency were not significantly different from those in saline ($P > 0.05$; Fig. 6d,f,g).

In contrast to MEPs, the SSEP amplitude showed a clear and time-dependent decrease in the 10 mM and 20 mM QX-314/0.05% capsaicin groups, with suppression observed as early as 10 min and continuing through 30 min (Fig. 6b,c, right). At 30 min, both the 10 mM and 20 mM groups showed significantly decreased SSEP amplitudes compared with those in the saline group ($P < 0.0001$; Fig. 6e,f), while the SSEP latency remained unchanged ($P > 0.05$; Fig. 6e,g).

To evaluate recovery of this sensory-selective block, we recorded evoked potentials every 5 min after injection. SSEP amplitude gradually recovered and fully returned to baseline levels by 50 min post-injection, while MEPs remained stable throughout (Fig. 6h). To confirm that high-dose 20 mM QX-314/capsaicin treatment did not cause nerve injury, we performed hematoxylin-eosin (HE) staining on DRGs and sciatic nerves 50 min after injection. No visible signs of tissue damage were observed, when compared with saline controls (Supplementary Fig. S1e–h).

Together, these results demonstrate that the QX-314/capsaicin combination produces a selective and reversible block of sensory conduction without impairing motor function or causing structural nerve damage. Our MEP/SSEP-based in vivo model is effective for identifying such a differential nerve blockade.

Discussion

This study successfully developed a novel rat model based on MEPs and SSEPs for in vivo evaluation of the selective nerve blockade effects of local anesthetics. Through a systematic exploration of how physiological parameters (e.g., anesthesia, recording duration, temperature, and oxygen supply conditions) influence MEPs and SSEPs, we identified key factors for optimizing model stability, namely maintaining a normal body temperature (36–38 °C) and continuous oxygenation and controlling the measurement time within 1 h.

To validate the reliability of the model, we used lidocaine as a negative control. The experimental results were highly consistent with its pharmacological characteristics, as lidocaine significantly inhibited both MEPs and SSEPs, confirming its non-selective blockade of sensory and motor nerves (Fig. 7). Subsequently, we used the model to evaluate a combination of the novel local anesthetic QX-314 and capsaicin. The choice of this positive control was based on previous research[16–18], which demonstrated that this combination selectively blocks sensory nerves without affecting motor function. Mechanistically, QX-314 is a permanently charged quaternary derivative of lidocaine that cannot pass through cell membranes under physiological conditions[19]. However, when co-administered with capsaicin, a transient receptor potential vanilloid 1 (TRPV1) channel agonist, QX-314 can selectively enter nociceptive neurons via TRPV1 activation and subsequently block sodium channels from the intracellular side[16]. Capsaicin itself does not possess local anesthetic properties but rather acts as a molecular gate for QX-314 entry[16]. Therefore, most studies use a fixed concentration of capsaicin (typically 0.05%) while titrating QX-314 dosage to achieve selective sensory blockade. For example, prior studies have reported effective sensory blockade with 0.2% QX-314 + 0.05% capsaicin[20], 0.5% QX-314 + 0.05% capsaicin[21], and 1.0% QX-314 + 0.05% capsaicin[22], all without inducing motor deficits. This strategy also minimizes the risk of peripheral neurotoxicity from high concentrations of capsaicin[23–25]. Based on this rationale, we adopted two different QX-314 concentrations (10 mM and 20 mM) with a fixed capsaicin dose (0.05%) in our model. Our results supported that QX-314/capsaicin suppressed SSEPs but had no significant effect on MEPs (Fig. 7), consistent with previous reports, thus thoroughly demonstrating the accuracy and reliability of this model in assessing the selective blockade. Together with the non-selective effects of lidocaine, which served as a negative control, these results strongly validated that our model can distinguish between sensory-selective and non-selective local anesthetic agents in vivo.

This study holds significant clinical relevance. According to a report from *The Lancet* in 2017[27], over 300 million surgeries worldwide require anesthesia each year, with the vast majority relying on general anesthesia. However, postoperative pain management remains a serious challenge, as commonly used opioid medications and nonsteroidal anti-inflammatory drugs can cause various systemic side effects such as nausea, vomiting, and respiratory depression[27]. Development of local anesthetics that provide selective sensory blockade would not only provide effective postoperative pain control but also would preserve motor function, promoting early patient mobilization and reducing opioid consumption.

Compared with traditional behavioral assessment methods, this model offers significant advantages. MEPs and SSEPs can be used to directly record electrophysiological signals from nerve conduction, avoiding subjective biases in behavioral assessments[28]. Furthermore, this model has high sensitivity, allowing for the detection of subtle changes in nerve conduction that have not yet manifested as behavioral abnormalities. Unlike traditional methods that require animals to be awake and cooperative (such as thermal pain and mechanical pain tests), this model allows for recordings under full anesthesia, effectively avoiding interference from the experimental environment and the animal's behavior[6,8], significantly enhancing the reproducibility and reliability of the experiment.

Regarding model stability, previous studies have shown that various physiological factors, such as body temperature and hypoxia, can interfere with MEP and SSEP recordings[29–31], ultimately affecting the accuracy and reliability of experimental results. Moreover, different anesthetic agents also modulate evoked potentials in a dose-dependent manner[32–35]. Therefore, when using MEP and SSEP models to screen local anesthetics, a comprehensive monitoring and regulation system is essential to minimize these confounding influences and ensure reproducible data.

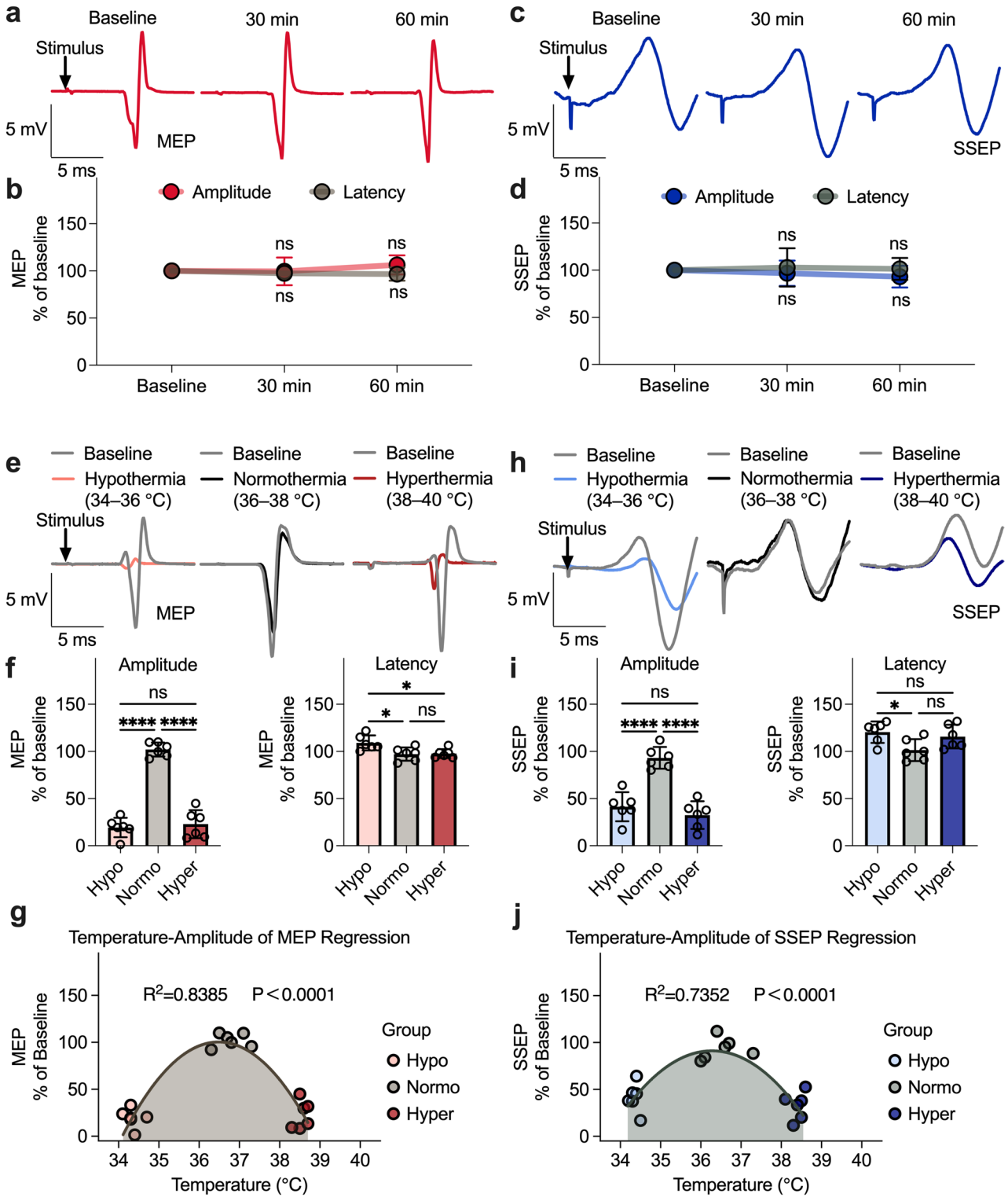

Based on this reason, we first investigated the impact of various anesthetic drugs on evoked potentials to identify a suitable anesthetic strategy. Our findings indicated that propofol can be used safely for continuous anesthesia during evoked potential recordings, provided that the infusion rate is carefully controlled (10–40 mg/kg/h). Additionally, it is important to note that the evaluation window in this model is limited to 1 h, which is based on the potential accumulation effects of propofol. While the propofol infusion doses we chose (10–40 mg/kg/h) are within the safe range, previous studies have shown that propofol significantly inhibits MEPs induced by single-pulse electrical stimulation[36], and high doses (1 mg/kg/min) may also affect evoked potentials[37]. Therefore, we recommend limiting the evaluation time to 1 h to ensure the robustness of the model.

Subsequently, we examined MEPs and SSEPs under different physiological conditions to identify optimal recording parameters. Consistent with previous research, our results confirm that body temperature and oxygenation significantly affect evoked potentials. Regarding the impact of temperature on nerve conduction,

◀**Fig. 3**. Stability of MEP and SSEP recordings over time and under different body temperatures. (**a,b**) Representative MEP waveforms and quantitative analysis showing stable amplitude and latency over a 60-minute period ($n = 6$). (**c,d**) Representative SSEP waveforms and quantification also confirm stable signals up to 60 min ($n = 6$). (**e,f**) MEP waveforms and quantitative results under hypothermia (34–36 °C), normothermia (36–38 °C), and hyperthermia (38–40 °C). Hypothermia and hyperthermia both significantly reduced MEP amplitude, and latency was prolonged under hypothermia ($n = 6$). (**g**) Non-linear regression analysis reveals a strong relationship between body temperature and MEP amplitude ($R^2 = 0.8385$, $P < 0.0001$). (**h,i**) Similar temperature effects were observed in SSEP: amplitude decreased significantly under hypo- and hyperthermia, while only hypothermia slightly increased latency ($n = 6$). (**j**) Non-linear regression analysis confirms a significant relationship between body temperature and SSEP amplitude ($R^2 = 0.7352$, $P < 0.0001$). Data are shown as mean ± SD. Statistical analysis: two-way ANOVA (**b**,**d**) and one-way ANOVA (**f**,**i**), and non-linear regression (**g**,**j**); statistical significance: ns = not significant, $^*P < 0.05$, $^{****}P < 0.0001$.

our findings differ somewhat from previous literature[29]. Previous reports suggest that extreme temperatures (> 42 °C or < 28 °C) significantly alter the latency and amplitude of MEPs and SSEPs, whereas our experiments did not reveal substantial changes in latency across our tested temperature ranges. This difference may stem from (1) our temperature settings being relatively mild and not reaching the threshold required to induce significant changes in latency; or (2) the use of 100% O_2 throughout the experiment, which may have alleviated the negative effects of temperature on nerve conduction. Nevertheless, maintaining a constant body temperature remains a critical factor in ensuring the stability of the model.

In summary, we have successfully developed and validated a novel rat model based on MEPs and SSEPs for in vivo evaluation of the selective nerve blockade effects of local anesthetics. After optimizing physiological parameters, such as the anesthetic dosage, recording duration, temperature, and oxygen supply, this model demonstrated excellent robustness and reliability. It offers a valuable experimental platform for the development of new local anesthetics designed to achieve sensory-motor separation.

Materials and methods

Animals

All animal procedures were approved by the Animal Ethics Committee of West China Hospital, Sichuan University (Approval No. 20241101011), and were carried out in accordance with institutional guidelines for the care and use of laboratory animals. All methods were performed in accordance with the relevant guidelines and regulations. This study is reported in accordance with the ARRIVE guidelines (https://arriveguidelines.org).

Adult male Sprague-Dawley rats weighing approximately 250–300 g were purchased from Dossy Biotechnology Co., Ltd. (Chengdu, China). All rats were housed individually in polypropylene cages (50 cm × 20 cm × 15 cm) for 1 week of acclimatization before the formal experiments. The animals were maintained at room temperature (24 °C ± 2 °C), with relative humidity of 50–55% and a 12:12-h light/dark cycle, with free access to food and water. During all surgical electrode implantation procedures, rats were placed on a temperature-controlled blanket system, and their body temperature was maintained at 37 °C ± 0.5 °C using a rectal probe. Erythromycin ointment was applied to the rats' eyes to prevent dryness.

Chemicals

QX-314 and lidocaine were purchased from Sigma-Aldrich Canada Ltd. (Oakville, ON, Canada). Capsaicin was purchased from Targetmol (T1062, Targetmol, Boston, MA, USA). For animal experiments, all drug solutions were prepared using ultrapure water from a Milli-Q integrated ultrapure water system (Merck Millipore, Darmstadt, Germany). Capsaicin was freshly prepared using a solvent consisting of 10% ethanol, 10% Tween 80, and 80% ultrapure water.

Electrode implantation

Following sevoflurane anesthesia (2.5% induction, 1.5–3% maintenance; O_2: 0.5–1.0 L/min), rats were fixed in a stereotaxic frame. A midline scalp incision was made to expose the skull. Five skull holes were drilled using a 1.2 mm dental drill, based on prior studies[32,33,38–40] and refined by our preliminary experiments, to target both the motor and sensory cortices.

For MEP stimulation, two screw electrodes were implanted into the left motor cortex (1.5 mm anterior and 2.5 mm lateral; 1.0 mm posterior and 1.5 mm lateral to Bregma). For SSEP recordings, two electrodes were placed in the left sensory cortex (1.0 mm posterior and 3.8 mm lateral; 2.5 mm posterior and 2.8 mm lateral to Bregma), and a reference electrode was placed 1.0 mm posterior and 3.0 mm lateral to Lambda.

All electrodes (1.4 mm diameter, 3.5 mm length) were inserted approximately 0.75 mm deep to lightly contact the dura without compression. Silver wires were welded to the bases, and dental cement was applied to fix the electrodes. After curing, the incision was sutured, and antibiotics were administered for 3 days. No complications were observed during the experiment. Post-mortem histology confirmed that no pathological changes such as hematomas or cortical compression were observed beneath the electrodes, indicating that this combined implantation method is both safe and reliable.

MEP recordings

Electrical pulses were delivered via a constant voltage stimulator connected to the skull electrodes using alligator clips. Signals were recorded using subcutaneous needle electrodes; the recording electrode was inserted into the right tibialis anterior muscle, the reference electrode was placed on the right hind paw, and the ground electrode

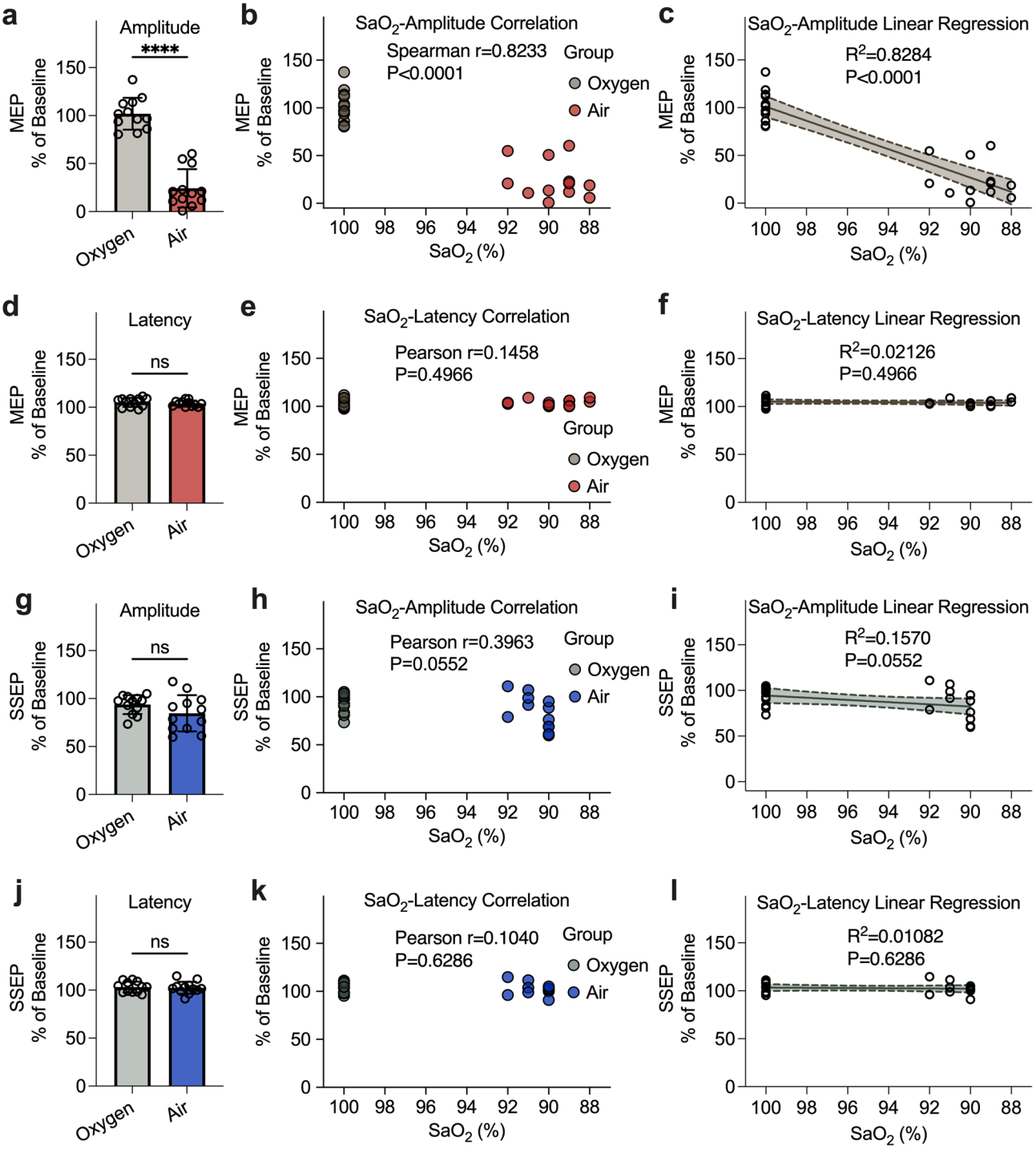

Fig. 4. Effects of oxygen supply conditions on MEP and SSEP amplitudes and latencies. (**a**,**d**) Compared to 100% oxygen, MEP amplitude was significantly reduced in rats breathing room air (21% O_2), while latency remained unchanged ($n = 6$). (**b**,**c**) MEP amplitude showed strong positive correlation with arterial oxygen saturation (SaO_2, Spearman $r = 0.8233$, $P < 0.0001$), and linear regression confirmed a robust association ($R^2 = 0.8284$, $P < 0.0001$). (**e**,**f**) MEP latency showed no correlation with SaO_2. (**g**,**j**) SSEP amplitude and latency were unaffected by oxygen levels ($n = 6$). (**h**,**i**,**k**,**l**) Although SSEP amplitude showed weak correlation with SaO_2 (Pearson $r = 0.3963$, $P = 0.0552$), regression analysis revealed low explanatory power ($R^2 = 0.1570$). Data are presented as mean ± SD. Statistical analysis: unpaired t-test (**a**,**d**,**g**,**j**), simple linear correlation (**b**,**e**,**h**,**k**) and regression (**c**,**f**,**i**,**l**); statistical significance: ns = not significant, $^{****}P < 0.0001$. SaO_2, arterial oxygen saturation.

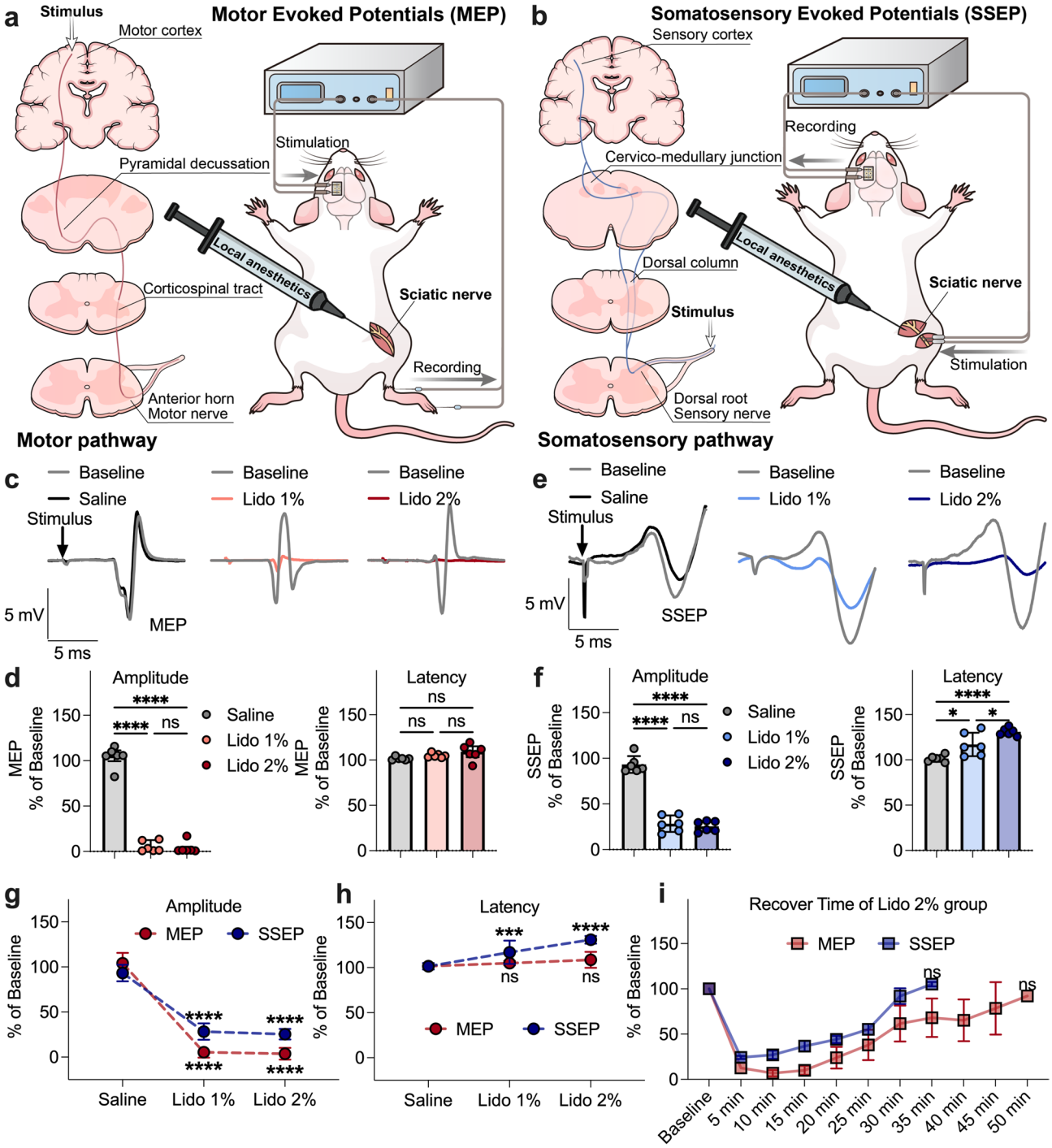

Fig. 5. Evaluation of lidocaine's non-selective nerve blockade. (**a,b**) Schematics showing administration of lidocaine and recording of MEP and SSEP after sciatic nerve exposure. (**c,d**) Representative MEP waveforms and quantitative analysis showing that both 1% and 2% lidocaine nearly abolished MEP amplitude, with no change in latency ($n = 6$). (**e,f**) SSEP amplitude was significantly reduced by lidocaine, with corresponding latency prolongation observed at higher concentrations ($n = 6$). (**g,h**) Combined plots illustrating that both sensory and motor pathways were equally suppressed by lidocaine, confirming its non-selective nerve blockade properties. (**i**) Recovery time course of MEP and SSEP amplitudes following perineural injection of 2% lidocaine, showing that signals for both pathways returned to baseline levels within 50 min ($n = 6$). Data are shown as mean ± SD. Statistical analysis: one-way ANOVA (**d,f**) and two-way ANOVA (**g,h,i**); statistical significance: ns = not significant, $^{*}P < 0.05$, $^{***}P < 0.001$, $^{****}P < 0.0001$. Lido, lidocaine.

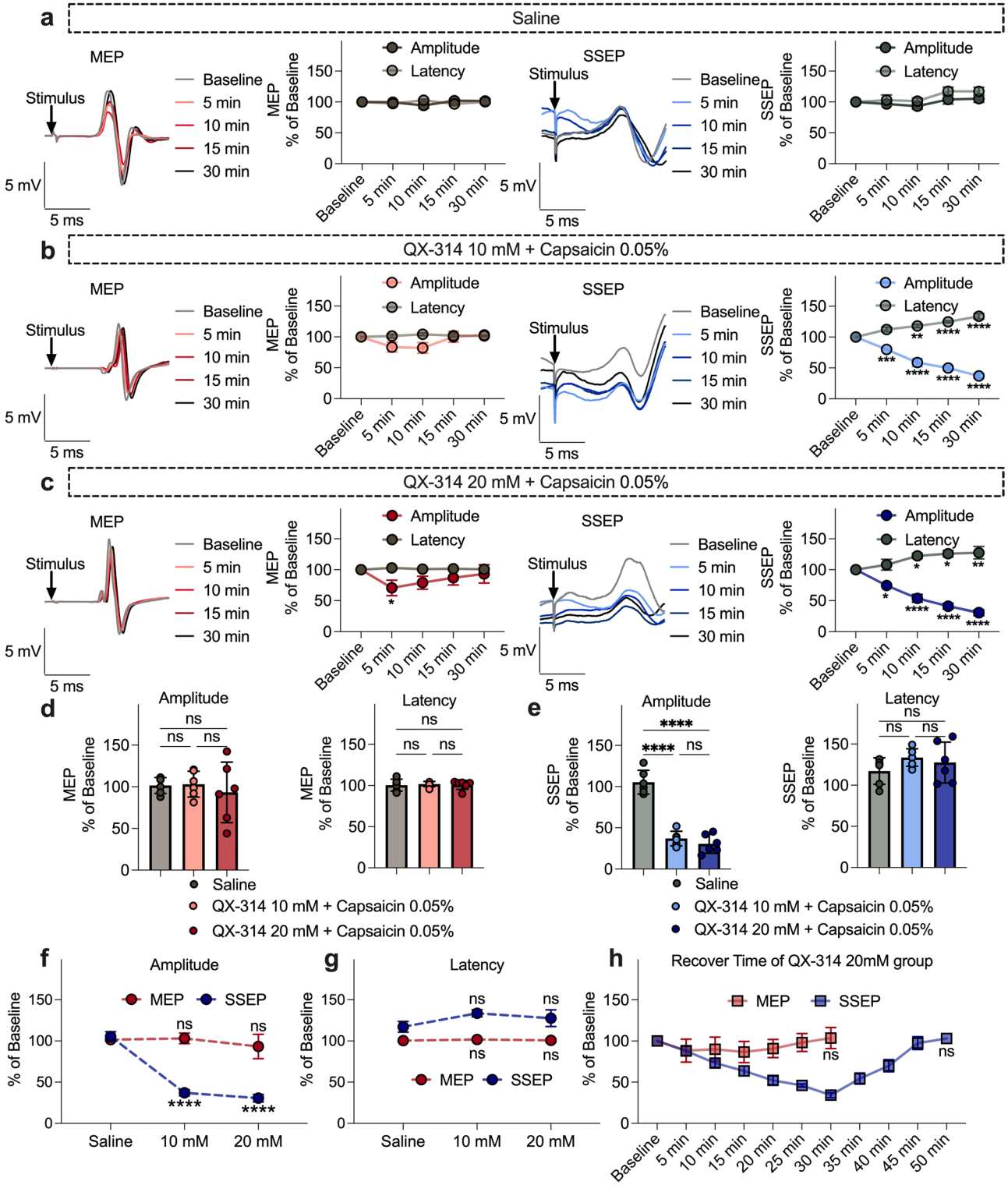

was inserted subcutaneously into the neck. Signals were amplified (10,000×), filtered (bandpass: 10–3000 Hz), and stored for subsequent analysis.

All recordings were performed in a Faraday cage to minimize electrical noise. The anesthetic depth was monitored by corneal and limb withdrawal reflexes to ensure stability. Electrical stimulation was applied using single pulses (0.6 ms, 0.1 Hz), with the intensity increased from 6 to 16 mV in 1 mV steps until the maximal MEP amplitude was reached. This threshold intensity was used for all subsequent trials. Each stimulation was repeated seven times, and signals were averaged for analysis.

After each pulse sequence, MEP signals were recorded for a 500 ms window, but only the initial 50 ms post-stimulus was analyzed. A 500 ms recording was also obtained to assess any high-latency changes, although no such changes were observed; therefore, only the 50 ms portion of the MEP signal was analyzed. A notch filter was used to remove 50 Hz noise from the signal, and the overlapped waveform was averaged, with each average

◀**Fig. 6**. Evaluation of selective nerve blockade by QX-314/capsaicin. (**a**) Saline treatment showed no change in MEP or SSEP amplitude and latency over 30 min ($n=6$). (**b**) Application of 10 mM QX-314 with 0.05% capsaicin suppressed SSEP amplitude progressively over time, with no significant changes in MEP ($n=6$). (**c**) Increasing the QX-314 concentration to 20 mM further reduced SSEP amplitude, still without affecting MEP ($n=6$). (**d**) Summary of 30 min time point showing no difference in MEP amplitude or latency across groups. (**e**) At 30 min, both 10 mM and 20 mM QX-314/capsaicin significantly reduced SSEP amplitude, while latency was mildly prolonged. (**f,g**) Comparative plots show the selective suppression of SSEP by QX-314/ capsaicin, confirming its sensory-selective nerve blockade effect. (**h**) Recovery time course following perineural injection of 20 mM QX-314/0.05% capsaicin, showing SSEP amplitude returning to baseline within 50 min while MEP amplitude remained stable throughout ($n=6$). Data are shown as mean ± SD. Statistical analysis: two-way ANOVA (**a**,**b**,**c**,**f**,**g**) and one-way ANOVA (**d**,**e**); statistical significance: ns = not significant, $^{**}P<0.01$, $^{***}P<0.001$, $^{****}P<0.0001$.

containing seven signal scans. The MEP latency was defined as the time from the stimulus artifact to the first deflection peak, and the amplitude was assessed by measuring the peak-to-trough value of the largest phase of the MEP waveform.

SSEP recordings

A lateral skin incision was made on the right femur, and the sciatic nerve was exposed via blunt muscle separation. A hook electrode coated with mineral oil, to reduce noise, was placed under the nerve for stimulation. Recordings were obtained from screw electrodes implanted in the left sensory cortex. The amplifier was set to a bandpass range of 20 to 1000 Hz. The analysis time window was 100 ms, and each SSEP waveform was averaged over 100 scans, meaning each signal represented the average of 100 repetitions. Recordings were conducted in a Faraday cage to reduce electrical noise. A notch filter was used to reduce power line interference.

Stimulation was delivered as single pulses (0.2 ms, 0.5 Hz) using constant current. The intensity was gradually increased from 3 to 8 mA until a visible twitch occurred, and the maximal SSEP amplitude was observed at the recording electrode. Stimuli were delivered at 2-second intervals to prevent signal decay. The minimal current required for the maximum amplitude was used for subsequent recordings. SSEP latency was defined as the time from stimulus onset to the first deflection peak, and the amplitude was measured from baseline to the peak.

Model condition screening

Anesthesia

Sedation was necessary for the rats during recording. Previous studies have shown that anesthetics/sedatives might be underlying interference factors in MEP and or SSEP recordings[32–34,41,42]. Therefore, selection of an appropriate anesthetic regimen is crucial to obtain reliable electrophysiological recordings. The present study aimed to identify the optimal anesthetic category and dosage for this model by investigating the dose effects of sevoflurane and propofol on MEPs and SSEPs. Specifically, MEPs and SSEPs were recorded before and after administering different sevoflurane concentrations and/or propofol doses (stabilized for 15–20 min at each dose/concentration). The percentage changes in amplitude and latency were calculated. The depth of anesthesia was assessed in real time by monitoring the corneal reflex and the limb withdrawal response to a painful stimulus, ensuring that an appropriate level of anesthesia was maintained while minimizing interference with the electrophysiological recordings.

Effects of physiological conditions on recording

Rats were randomly assigned to groups ($n=6$ per group) to assess how critical physiological factors influence MEP and SSEP recordings. Specifically, we evaluated (1) recording stability at different durations (baseline, 30 min, and 60 min); (2) the effects of temperature conditions, including hypothermia (34–36 °C), normothermia (36–38 °C), and hyperthermia (38–40 °C); and (3) the influence of oxygen supply conditions, comparing continuous oxygen supplementation (100% O_2) with room air (21% O_2).

Validation of selective nerve blockade

Selective nerve blockade was validated using local anesthetics/analgesics with well-known selectivity profiles. Specifically, lidocaine (1% and 2%) was used as a non-selective local anesthetic that blocks both sensory and motor conduction, and QX-314 combined with capsaicin (10 mM QX-314/0.05% capsaicin and 20 mM QX-314/0.05% capsaicin) was used as a sensory-selective agent[20,22,43].

A surgical exposure method was employed to precisely deliver anesthetics to the rat sciatic nerve[44]. Briefly, the sciatic nerve was exposed through a small incision between the femoral greater trochanter and the ischial tuberosity, followed by gentle muscle separation. Then, a micro-syringe containing 100 µL of anesthetic solution was used to directly administer the contents onto the nerve surface. This method localized the anesthetic to the vicinity of the exposed nerve. Notably, nerve stimulation for SSEPs was applied at the distal end of the nerve near the drug administration site, ensuring that the local anesthetic acted between the stimulation point and the central recording electrodes (Fig. 5a,b). This arrangement enabled clear differentiation of whether sensory or motor conduction pathways were blocked by the anesthetic intervention. By simultaneously recording MEPs and SSEPs, this design clearly distinguished sensory-selective blockade from non-selective nerve blockade.

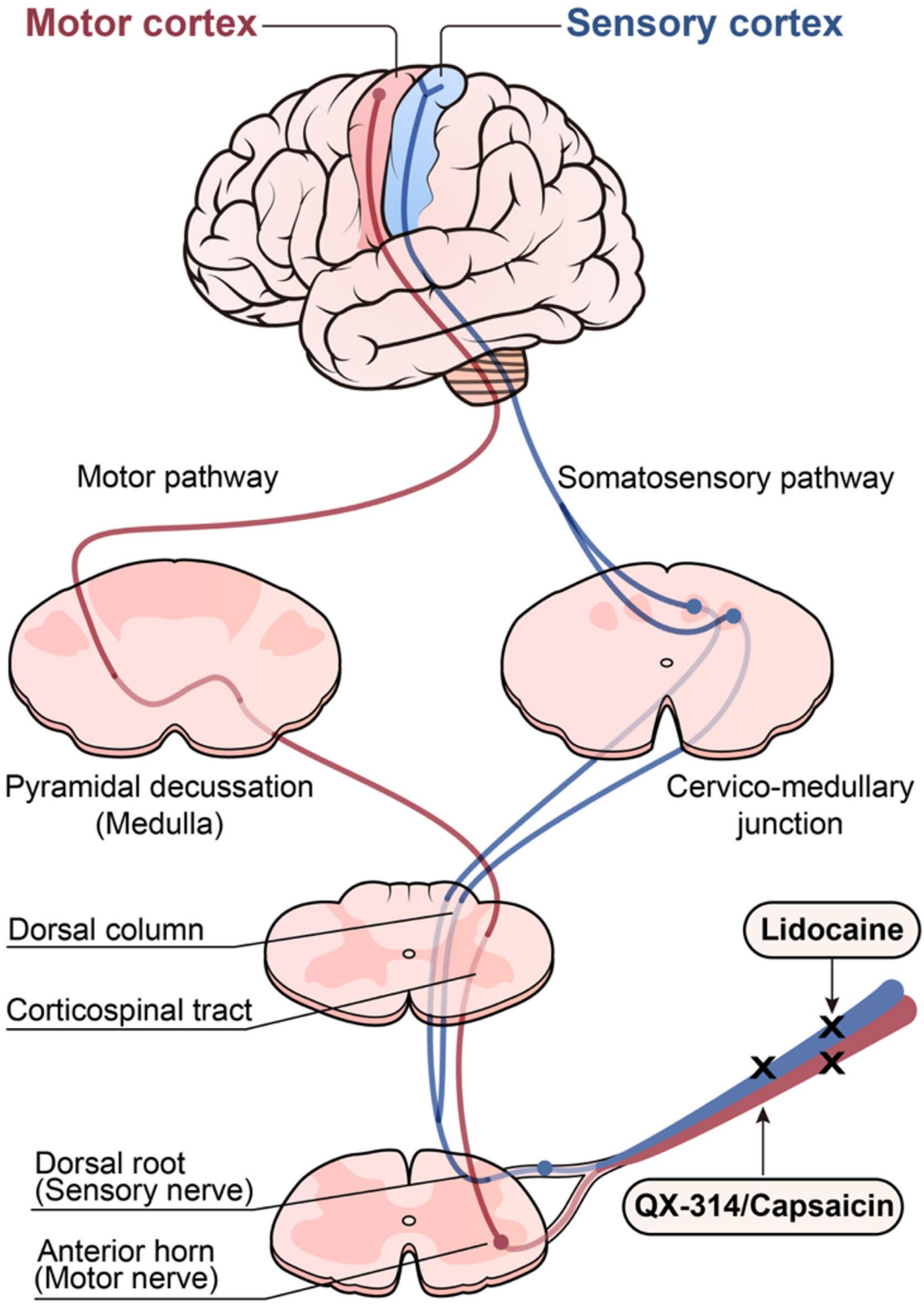

Fig. 7. Differential blockade of motor and sensory pathways. This figure shows a schematic of two different pathways. The motor (red) pathway travels from the cortex, down the spinal cord, and out to the muscles. The sensory (blue) pathway runs from the periphery, through the spinal cord, and up to the sensory cortex. Lidocaine blocks both pathways, inhibiting MEPs and SSEPs, showing its non-selective blockade effect. In contrast, QX-314/capsaicin selectively blocks the sensory pathway, suppressing SSEPs but sparing MEPs. This model helps distinguish between selective and non-selective blockade of motor and sensory nerves by different local anesthetics.

Assessment of neurotoxicity and recovery after nerve blockade

To evaluate the potential neurotoxicity of high-dose local anesthetics and to confirm the reversibility of nerve blockade, we assessed both electrophysiological recovery and histological changes following administration of 2% lidocaine and 20 mM QX-314/0.05% capsaicin. After the complete suppression of MEPs and/or SSEPs, signals were continuously recorded every 5 min until the evoked potentials fully recovered, in order to monitor functional recovery. Rats were then euthanized immediately, and the ipsilateral sciatic nerve and L4–L6 dorsal root ganglia (DRGs) from the drug-treated side were harvested. Tissues were fixed in 4% paraformaldehyde, embedded in paraffin, and cut into 5 μm-thick sections. Hematoxylin-eosin (HE) staining was performed to evaluate histological integrity, including assessment of inflammatory cell infiltration and axonal integrity.

Data collection and analysis

The latencies and amplitudes of MEPs and SSEPs under different physiological conditions and drug interventions were recorded, and the percentage changes in amplitude and latency were calculated. Statistical analysis was performed using GraphPad Prism 10.4.1 (San Diego, California, USA). The Shapiro–Wilk test was used to verify the normality assumption of the data, and continuous data are presented as the mean ± standard deviation. Paired t-tests were used for group comparisons, and one-way or two-way ANOVA was used for multiple comparisons to analyze the effects of recording duration, temperature, oxygen conditions, and drugs on MEPs and SSEPs. Differences were considered significant when the P-value was less than 0.05.

Data availability

Data will be made available from the corresponding author on request.

Received: 30 April 2025; Accepted: 15 July 2025
Published online: 20 July 2025

References

1. Lirk, P., Picardi, S. & Hollmann, M. W. Local anaesthetics: 10 essentials. *Eur. J. Anaesthesiol.* **31**, 575–585 (2014).
2. Vadhanan, P., Tripaty, D. K. & Adinarayanan, S. Physiological and pharmacologic aspects of peripheral nerve blocks. *J. Anaesthesiol. Clin. Pharmacol.* **31**, 384–393 (2015).
3. Sinatra, R. S., Torres, J. & Bustos, A. M. Pain management after major orthopaedic surgery: current strategies and new concepts. *J. Am. Acad. Orthop. Surg.* **10**, 117–129 (2002).
4. Milligan, K. R. Recent advances in local anaesthetics for spinal anaesthesia. *Eur. J. Anaesthesiol.* **21**, 837–847 (2004).
5. Hargreaves, K., Dubner, R., Brown, F., Flores, C. & Joris, J. A new and sensitive method for measuring thermal nociception in cutaneous hyperalgesia. *Pain*. **32**, 77–88 (1988).
6. Amaya, F. et al. The voltage-gated sodium channel Na(v)1.9 is an effector of peripheral inflammatory pain hypersensitivity. *J. Neurosci.* **26**, 12852–12860 (2006).
7. Simon, D. et al. Friedreich ataxia mouse models with progressive cerebellar and sensory ataxia reveal autophagic neurodegeneration in dorsal root ganglia. *J. Neurosci.* **24**, 1987–1995 (2004).
8. Templin, J. S. et al. Neosaxitoxin in rat sciatic block: improved therapeutic index using combinations with bupivacaine, with and without epinephrine. *Anesthesiology*. **123**, 886–898 (2015).
9. Jameson, L. C. & Sloan, T. B. Monitoring of the brain and spinal cord. *Anesthesiol. Clin.* **24**, 777–791 (2006).
10. Gonzalez, A. A., Jeyanandarajan, D., Hansen, C., Zada, G. & Hsieh, P. C. Intraoperative neurophysiological monitoring during spine surgery: a review. *Neurosurg. Focus*. **27**, E6 (2009).
11. Charalampidis, A. et al. The use of intraoperative neurophysiological monitoring in spine surgery. *Glob. Spine J.* **10**, 104S–114S (2020).
12. Tropeano, M. P. et al. Multimodal intraoperative neurophysiological monitoring in intramedullary spinal cord tumors: A 10-Year single center experience. *Cancers (Basel)*. **16**, 111 (2023).
13. Scibilia, A. et al. Intraoperative neurophysiological mapping and monitoring in spinal tumor surgery: sirens or indispensable tools? *Neurosurg. Focus*. **41**, E18 (2016).
14. Alkire, M. T., McReynolds, J. R., Hahn, E. L. & Trivedi, A. N. Thalamic microinjection of nicotine reverses sevoflurane-induced loss of righting reflex in the rat. *Anesthesiology*. **107**, 264–272 (2007).
15. Wang, Y. et al. Effects of propofol on the dopamine, metabolites and GABAA receptors in media prefrontal cortex in freely moving rats. *Am. J. Transl. Res.* **8**, 2301–2308 (2016).
16. Binshtok, A. M., Bean, B. P. & Woolf, C. J. Inhibition of nociceptors by TRPV1-mediated entry of impermeant sodium channel blockers. *Nature* **449**, 607–610 (2007).
17. Roberson, D. P., Binshtok, A. M., Blasl, F., Bean, B. P. & Woolf, C. J. Targeting of sodium channel blockers into nociceptors to produce long-duration analgesia: a systematic study and review. *Br. J. Pharmacol.* **164**, 48–58 (2011).
18. Gerner, P. et al. Capsaicin combined with local anesthetics preferentially prolongs sensory/nociceptive block in rat sciatic nerve. *Anesthesiology*. **109**, 872–878 (2008).
19. Chernoff, D. M. & Strichartz, G. R. Kinetics of local anesthetic inhibition of neuronal sodium currents. pH and hydrophobicity dependence. *Biophys. J.* **58**, 69–81 (1990).
20. Binshtok, A. M. et al. Coapplication of Lidocaine and the permanently charged sodium channel blocker QX-314 produces a long-lasting nociceptive Blockade in rodents. *Anesthesiology*. **111**, 127–137 (2009).
21. Brenneis, C. et al. Phenotyping the function of TRPV1-expressing sensory neurons by targeted axonal Silencing. *J. Neurosci.* **33**, 315–326 (2013).
22. Zhou, C. et al. Emulsified isoflurane enhances thermal transient receptor potential vanilloid-1 channel activation–mediated sensory/nociceptive Blockade by QX-314. *Anesthesiology*. **121**, 280–289 (2014).
23. Shankarappa, S. A. et al. Duration and local toxicity of sciatic nerve blockade with coinjected site 1 sodium-channel blockers and quaternary lidocaine derivatives. *Reg. Anesth. Pain Med.* **37**, 483–489 (2012).
24. Welk, E., Petsche, U., Fleischer, E. & Handwerker, H. O. Altered excitability of afferent C-fibres of the rat distal to a nerve site exposed to capsaicin. *Neurosci. Lett.* **38**, 245–250 (1983).
25. Schwarz, S. K. W. et al. Lumbar intrathecal administration of the quaternary Lidocaine derivative, QX-314, produces irritation and death in mice. *Anesthesiology*. **113**, 438–444 (2010).
26. GBD 2017 Disease and Injury Incidence and Prevalence Collaborators. Global, regional, and National incidence, prevalence, and years lived with disability for 354 diseases and injuries for 195 countries and territories, 1990–2017: a systematic analysis for the global burden of disease study 2017. *Lancet*. **392**, 1789–1858 (2018).

27. Szekeres, M. Management of postoperative pain. *J. Physiother*. **64**, 62 (2018).
28. Møller, A. R., Ansari, S. & Cohen-Gadol, A. A. Techniques of intraoperative monitoring for spinal cord function: their past, present, and future directions. *Neurol. Res.* **33**, 363–370 (2011).
29. Oro, J. & Haghighi, S. S. Effects of altering core body temperature on somatosensory and motor evoked potentials in rats. *Spine (Phila Pa. 1976)*. **17**, 498–503 (1992).
30. Haghighi, S. S., Keller, B. P., Oro, J. J. & Gibbs, S. R. Motor-evoked potential changes during hypoxic hypoxia. *Surg. Neurol.* **39**, 399–402 (1993).
31. Grundy, B. L., Heros, R. C., Tung, A. S. & Doyle, E. Intraoperative hypoxia detected by evoked potential monitoring. *Anesth. Analg.* **60**, 437–439 (1981).
32. Zandieh, S., Hopf, R., Redl, H. & Schlag, M. G. The effect of ketamine/xylazine anesthesia on sensory and motor evoked potentials in the rat. *Spinal Cord*. **41**, 16–22 (2003).
33. Kortelainen, J., Al-Nashash, H., Vipin, A., Thow, X. Y. & All, A. The effect of anaesthesia on somatosensory evoked potential measurement in a rat model. *Lab. Anim*. **50**, 63–66 (2016).
34. Keller, B. P., Haghighi, S. S., Oro, J. J. & Eggers, G. W. The effects of propofol anesthesia on transcortical electric evoked potentials in the rat. *Neurosurgery*. **30**, 557–560 (1992).
35. Kumar, A., Bhattacharya, A. & Makhija, N. Evoked potential monitoring in anaesthesia and analgesia. *Anaesthesia*. **55**, 225–241 (2000).
36. Kalkman, C. J. et al. Effects of propofol, etomidate, midazolam, and fentanyl on motor evoked responses to transcranial electrical or magnetic stimulation in humans. *Anesthesiology*. **76**, 502–509 (1992).
37. Oria, M., Chatauret, N., Raguer, N. & Córdoba, J. A new method for measuring motor evoked potentials in the awake rat: effects of anesthetics. *J. Neurotrauma*. **25**, 266–275 (2008).
38. Bhattacharyya, S., Kochhar, K. P. & Jain, S. Recording of motor and somatosensory evoked potential in an anaesthetised Wistar rat using digital polyrite system. *IJPP*. **66**, 98–102 (2022).
39. Schlag, G., Hopf, R. & Redl, H. Serial recording of sensory, corticomotor, and brainstem-derived motor evoked potentials in the rat. *Somatosens. Motor Res.* **18**, 106–116 (2001).
40. All, A. H., Nashash, A., Mir, H., Luo, H., Liu, X. & S. & Characterization of transection spinal cord injuries by monitoring somatosensory evoked potentials and motor behavior. *Brain Res. Bull.* **156**, 150–163 (2020).
41. Haghighi, S. S. Influence of isoflurane anesthesia on motor evoked potentials elicited by transcortical, brainstem, and spinal root stimulation. *Neurol. Res.* **20**, 555–558 (1998).
42. Haghighi, S. S., Green, K. D., Oro, J. J., Drake, R. K. & Kracke, G. R. Depressive effect of isoflurane anesthesia on motor evoked potentials. *Neurosurgery*. **26**, 993–997 (1990).
43. Sagie, I. & Kohane, D. S. Prolonged sensory-selective nerve blockade. *Proc. Natl. Acad. Sci.* **107**, 3740–3745 (2010).
44. Hung, Y. C. et al. Magnesium sulfate diminishes the effects of amide local anesthetics in rat sciatic-nerve block. *Reg. Anesth. Pain Med.* **32**, 288–295 (2007).

Acknowledgements

We thank Qingchao Fan and Huaqi Gan from the Research Center of Anesthesiology, West China Hospital of Sichuan University, for their help in electrode implantation.

Author contributions

Y.T., X.Z., C.Z., and M.O. conceptualized the study; Y.T. and X.Z. curated the data; Y.T., X.Z., and X.H. provided the methodology and performed the experiments; Y.T. and X.Z. wrote the original draft; J.L., C.Z. and M.O. edited the manuscript. All authors reviewed the manuscript.

Funding

This study was supported by grant No. 82371280 (to M.O.) and 82271290 (to C.Z.) from the National Natural Science Foundation of China and No. 2023NSFSC1565 (to M.O.) and 2023ZYD0168 (to C.Z.) from the Science and Technology Department of Sichuan Province, China.

Declarations

Competing interests

The authors declare no competing interests.

Additional information

Supplementary Information The online version contains supplementary material available at https://doi.org/10.1038/s41598-025-12201-5.

Correspondence and requests for materials should be addressed to M.O.